Design, Trade-Off and Advantages of a Reconfigurable Dual Reflector for Ku Band Applications

Cecilia Cappellin, Knud Pontoppidan

TICRA
Læderstræde 34
1201 Copenhagen
Denmark
Email:cc@ticra.com, kp@ticra.com

INTRODUCTION

Shaped reflectors form one of the cornerstones of satellite telecommunications today, and have in all but a few cases replaced the array-fed parabolic reflector antennas for contoured beam generation. The evolution started in the 1990'es with the advent of efficient and reliable software to generate the desired reflector profile on the basis of the requirements to the orbital position of the satellite and the desired coverage areas on the ground.
The increased in orbit lifetime of today's telecommunication satellites combined with the rapid development of the offered services require always more flexible payloads. In this context, the existence of antennas that can be reconfigured in orbit, and thus accommodate future service scenarios, has recently attracted the interest of the international community. The benefits of such antennas are several: allowing the use of the same spacecraft at several orbital locations, changing the coverages during the satellite lifetime, and compensating for varying weather conditions. Though extremely attractive in terms of cost and manufacturing, shaped reflectors lack so far the capability of being reconfigured in orbit, while this feature can be obtained by an array-fed parabolic reflector, provided the beam-forming network of the array is equipped with variable power dividers and phase shifters.

Several examples of possible reconfigurable shaped reflectors were studied over the years [1]-[4]. Though important and fundamental conclusions could be drawn from them, these past investigations have dealt with single offset reflectors and simple theoretical coverages. There was a need to consider a realistic mission scenario and antenna configuration, in order to clarify the reconfigurability that could be achieved in real life. In particular, when considering a dual reflector system, the advantages provided by a reconfigurable subreflector, as opposed to the much larger main reflector, needed to be quantified. This could be particularly interesting for typical Ku band communications antennas, where the sub reflector is around 0.3-0.6 m in diameter, while the main reflector can be in the range 1.2-2.5 m. The answer to this question can have significant implications on further development programs, and it is therefore important to have a clear understanding of where to concentrate the efforts.

The purpose of the present work is to study and quantify the properties, advantages and limitations provided by a shaped dual reflector equipped with a reconfigurable surface when applied to a realistic mission scenario in Ku band. Mechanical repointing of the antenna will be assumed. While preliminary results with traditional splines shaping have been reported in [5], we will here show the performances that can be achieved when the reconfigurable surface is modeled by a mesh of interwoven flexible wires with circular cross section, supported by a number of control points and with a free rim [4]. The performances of the reconfigurable shaped reflector will be compared to the ones of a traditional fixed shaped reflector designed to illuminate the envelope of the desired coverages and of a shaped but fixed dual reflector optimized for each individual coverage. The necessary number of actuators will be investigated and a sensitivity analysis to the actuator settings will be performed. Specific actuators failures will be also taken into account. In particular, the effects of an actuator which is stuck or free to move will be studied.

INTERCONTINENTAL MISSION SCENARIO

The scenario under investigation is the so-called Intercontinental mission suggested by Thales Alenia Space (TAS). It is constituted by three coverages, one over Central Africa (B_1+B_2), one over South Africa ($C_1+C_2+C_3$), and one over Russia (D_1+D_2), see Figure 1. The coverages are illuminated by a geostationary satellite which can be located between 10E and 70E. The directivity required over the coverages is given in Table 1. A minimum XPD of 30 dB and a beam pointing error of 0.12° shall be considered, while no isolation constraints are expected. The antenna shall work in Tx/Rx case in the frequency bands Tx=10.95-12.50 GHz and Rx=13.75-14.5 GHz. In general, reconfigurability is foreseen 18 times in the satellite life time (approximately once a year) and is required both in varying the satellite orbital location and in switching from one coverage to the other.
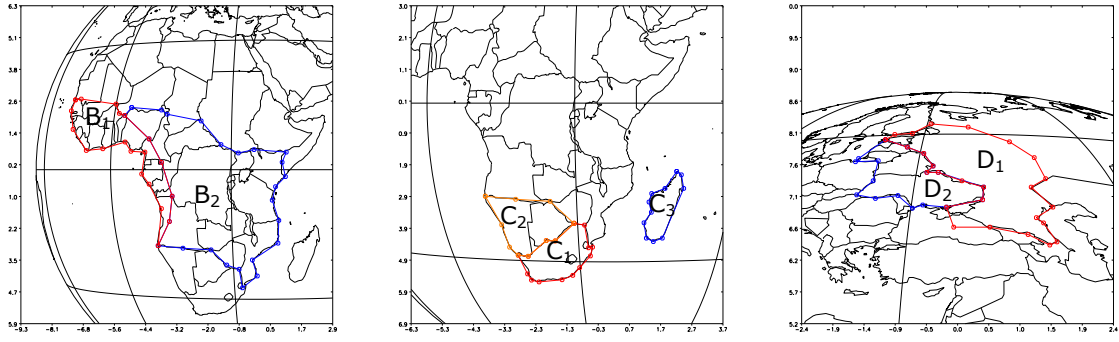
Figure 1. Polygons B_1, B_2, C_1, C_2 and C_3 and D_1 and D_2 seen from 36E.

Table 1. Directivity requirements for the coverages B_1+B_2, $C_1+C_2+C_3$ and D_1+D_2.

Polygon and antenna directivity		Polygon and antenna directivity		Polygon and antenna directivity	
B_1	Ref	C_1	Ref	D_1	Ref
B_2	Ref - 4 dB	C_2	Ref - 1 dB	D_2	Ref - 4 dB
		C_3	Ref - 7 dB		

ANTENNA OPTICAL SYSTEM

A dual offset Gregorian reflector antenna mounted on the spacecraft lateral side generates all coverages. The main reflector consists of a paraboloid in the *xyz*-coordinate system (CS), with circular projected aperture of diameter $D = 2.4$ m, focal length $f = 2.4$ m and clearance $d' = 0.3$ m, see Figure 2. The subreflector is an ellipsoid with circular projected aperture $D_2 = 0.8$ m. The Mizuguchi condition is applied.
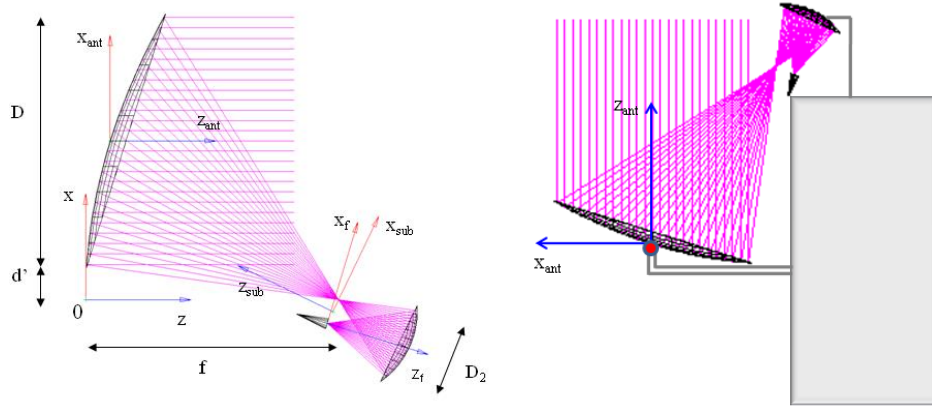
Figure 2. Dual reflector geometry and coordinate systems definition (on the left) and antenna mounted on the satellite lateral side with the RPM indicated.

The feed is linearly polarized along x_f and y_f, where $x_f y_f z_f$ is the feed CS, with origin at the second focal point of the ellipsoid, z_f pointing towards the center of the subreflector and x_f lying on the *xz*-plane. It is described by a Spherical Wave Expansion (SWE) in *ab*-modes provided by Thales at the frequencies of interest. The antenna CS is defined by $x_{ant} y_{ant} z_{ant}$, parallel to the *xyz*-CS and with origin at the center point of the main reflector surface. A reflector pointing mechanism (RPM) is assumed at the center of the main reflector.

OPTIMIZATION RESULTS

With the purpose of limiting the number of optimizations but at the same time investigating the largest number of parameters, a single orbital location (36E) is considered. Five frequencies (10.95, 11.7, 12.5, 13.75 and 14.5 GHz) and only one polarization (x_f) of the feed are taken into account.

The satellite CS $x_s y_s z_s$ is first identified, with origin at the satellite location, x_s-axis towards West, y_s-axis towards North and z_s-axis pointing towards the sub-satellite point on the Earth, see Figure 3. Initially, the antenna CS coincides with the satellite CS. The coverages are written in the satellite CS and the approximate center of each coverage (u_i,v_i) with $i =1,2,3$ is determined. It is reminded that the antenna can only provide service to one coverage at the time. The approximate center of gravity (u_g,v_g) of all the coverages is then found and the antenna CS is thus rotated by the corresponding (θ_g,φ_g) relative to its initial position in such a way that the entire antenna points towards (u_g,v_g). The feed

and the subreflector are fixed in this position once mounted on the satellite lateral face, see Figure 2, while the main reflector is tilted towards the midpoint between (u_g,v_g) and (u_i,v_i), depending on the coverage the antenna has to generate, to make the field radiated by the dual reflector antenna pointing towards (u_i,v_i). Far-field results and coverage polygons will be expressed in the following in the satellite CS. Three different cases will be shown.
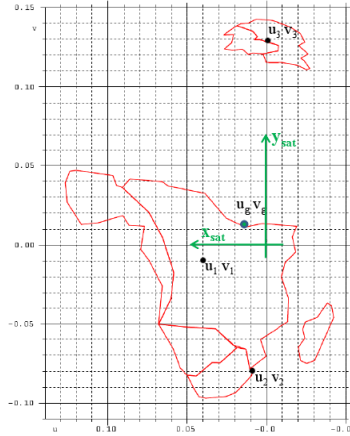
Figure 3. Polygon coverages in the satellite CS and their centers (u_i,v_i) and the center of gravity (u_g,v_g) highlighted.

Shaped subreflector and shaped main reflector for each individual coverage

The main reflector equipped by RPM and the subreflector were initially both shaped over each individual coverage, providing the best possible design for a shaped, but not reconfigurable, dual reflector optimized for each coverage. These results are used as reference in the following sections. The optimization was performed with the software POS5 [6] with the well-established spline modeling in order to satisfy the requirements on directivity and XPD on the coverages. On the basis of the main reflector size and the convergence mechanism, 30x30 and 12x12 splines were chosen to shape the main reflector and the subreflector respectively on each coverage. The minimum directivity obtained over the coverages is given in Table 2 and the amplitude of the co-polar component of the obtained far-fields together with the polygons in the satellite CS is shown in Figure 4. It is seen that contour levels agree very well with the desired regions and that obviously a higher directivity can be obtained over the smaller coverages.

Table 2. Directivity obtained for the coverages B_1+B_2, $C_1+C_2+C_3$ and D_1+D_2 with 30x30 splines for the main reflector and 12x12 splines for the subreflector on each individual coverage.

Polygon and antenna directivity		Polygon and antenna directivity		Polygon and antenna directivity	
B_1	30.9 dBi	C_1	34.5 dBi	D_1	36.1 dBi
B_2	26.9 dBi	C_2	33.5 dBi	D_2	32.1 dBi
		C_3	27.5 dBi		
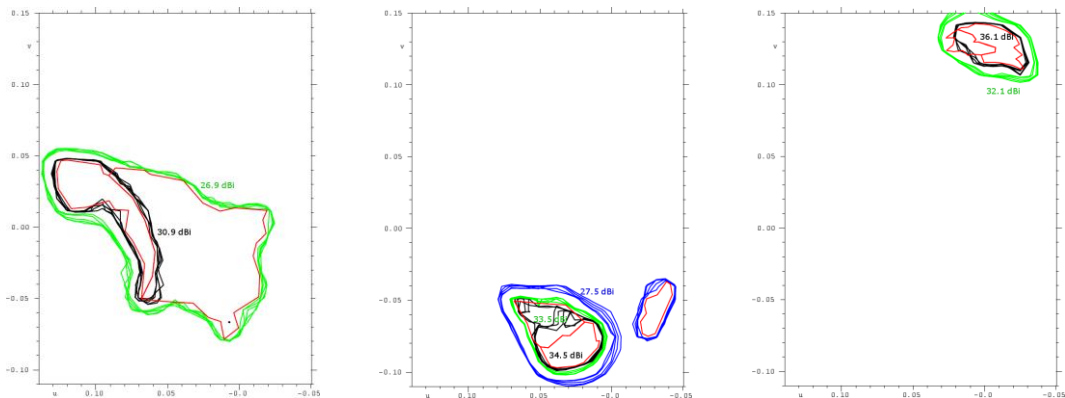
Figure 4. Coverage polygons (red curve) and amplitude of the co-polar component (minimum levels) of the obtained far-field in dBi in the satellite CS.

Ellipsoidal subreflector and shaped fixed main reflector

A traditional fixed main reflector shaped to maximize at the same time the minimum directivity on all the coverages was then analyzed. This represents the best and only possible solution when reconfigurability of the antenna cannot be achieved. Again, 30x30 splines were chosen to shape the main reflector, while the subreflector was kept ellipsoidal. The new directivity levels obtained over the coverage regions are given in Table 3, while the contour plots of the amplitude of the co-polar component of the obtained far-fields are shown in Figure 5. It is seen that 2.9 dB over B_1+B_2, 4 dB over $C_1+C_2+C_3$ and 4.1 dB over D_1+D_2 are lost relative to the optimum case of Table 2.

Table 3. Directivity obtained for the coverages B_1+B_2, $C_1+C_2+C_3$ and D_1+D_2 with 30x30 splines for the fixed main reflector and an ellipsoidal subreflector.

Polygon and antenna directivity		Polygon and antenna directivity		Polygon and antenna directivity	
B_1	28 dBi	C_1	30.5 dBi	D_1	32 dBi
B_2	24 dBi	C_2	29.5 dBi	D_2	28 dBi
		C_3	23.5 dBi		
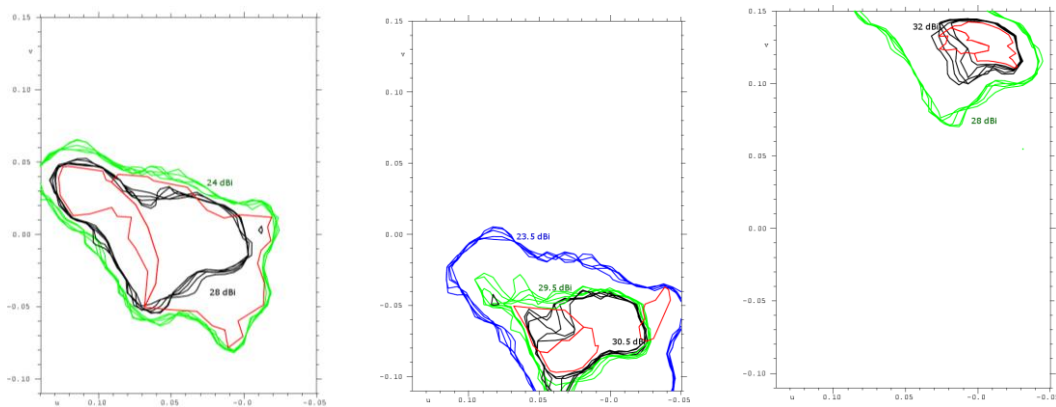
Figure 5. Coverage polygons (red curve) and amplitude of the co-polar component (minimum levels) of the obtained far-field in dBi in the satellite CS.

Reconfigurable subreflector and shaped fixed main reflector

The performances given by a shaped but fixed main reflector and a reconfigurable subreflector, optimized for each individual coverage, were finally investigated. The main reflector was fixed and shaped to provide, in case of ellipsoidal subreflector, a beam over the Earth given by a circle of radius 0.1 in the *uv*-coordinate system. This was considered a good general main reflector which can be used when the coverages to be illuminated are not predefined but are free to assume during the satellite lifetime arbitrary shapes. The main reflector was kept fixed while the subreflector was reconfigurable and shaped with a wire mesh of interwoven wires controlled by 55 actuators, placed on a triangular grid with a spacing along the *x*-direction of 10 cm, see Figure 6.
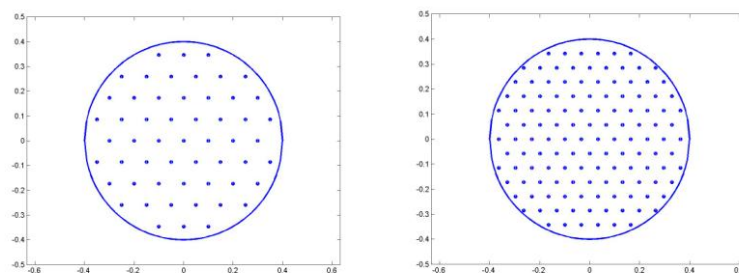
Figure 6. Position of the actuators over the subreflector projected aperture: 55 actuators on the left and 130 actuators on the right.

The obtained directivity levels are reported in Table 4 and the amplitude of the co-polar component of the far-fields is shown in Figure 7. It is observed that the obtained directivities differ from the optimum levels of Table 2 by 1.9 dB over B_1+B_2, 1.4 dB over $C_1+C_2+C_3$, and 1.2 over D_1+D_2. The possibility of reconfiguring the subreflector shape for every coverage, by using a fixed and general shaped main reflector, constitutes a very good improvement relative to the traditional performances reported in Table 3. While over the big coverage B_1+B_2 the directivity is only 1 dB higher, 2.6 dB and 2.9 dB are gained over the smaller coverages $C_1+C_2+C_3$ and D_1+D_2 respectively. It was found that directivity levels obtained by using N_i actuators are equivalently obtained by splines over the reconfigurable surface if the number

of splines is chosen according to $splines \approx \sqrt{2N_i}$, being *splines* the number used over the reconfigurable surface. In the present case, 12x12 splines over the subreflector provided the same directivity results given by 55 actuators.

Table 4. Directivity obtained for the coverages B_1+B_2, $C_1+C_2+C_3$ and D_1+D_2 for a general fixed main reflector and 55 actuators over the reconfigurable subreflector.

Polygon and antenna directivity		Polygon and antenna directivity		Polygon and antenna directivity	
B_1	29.0 dBi	C_1	33.1 dBi	D_1	34.9 dBi
B_2	25.0 dBi	C_2	32.1 dBi	D_2	30.9 dBi
		C_3	26.1 dBi		
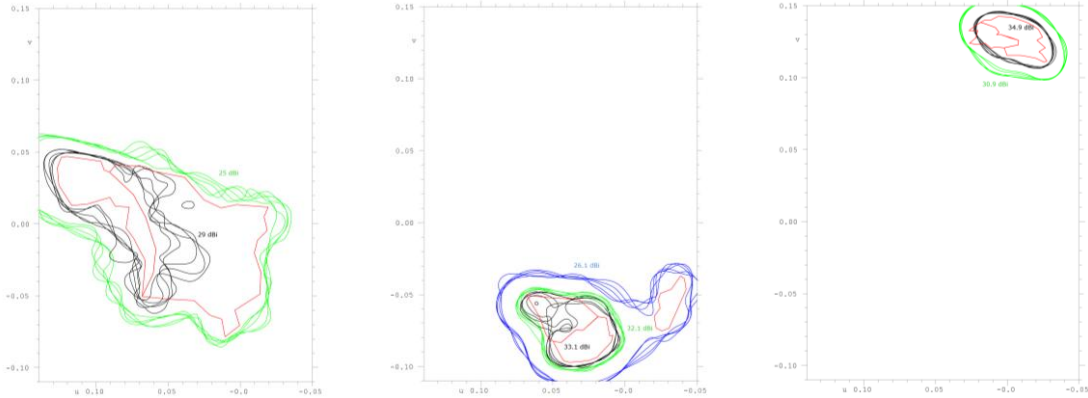
Figure 7. Coverage polygons (red curve) and amplitude of the co-polar component (minimum levels) of the obtained far-field in dBi in the satellite CS.

The subreflector shaping relative to the parental ellipsoid in the subreflector CS is shown in Figure 8. It is possible to see that, while lower values may be observed on the rim, the *z*-coordinates of the actuators lie in the range [-14 mm : 10 mm] and that the difference between the surfaces, at the actuator positions, is contained in the interval [-13 mm : 12 mm]. It was finally computed that by increasing the number of actuators to 130, see Figure 6, directivities could improve by 0.7 dB over B_1+B_2 but only 0.1 dB over $C_1+C_2+C_3$ and D_1+D_2.
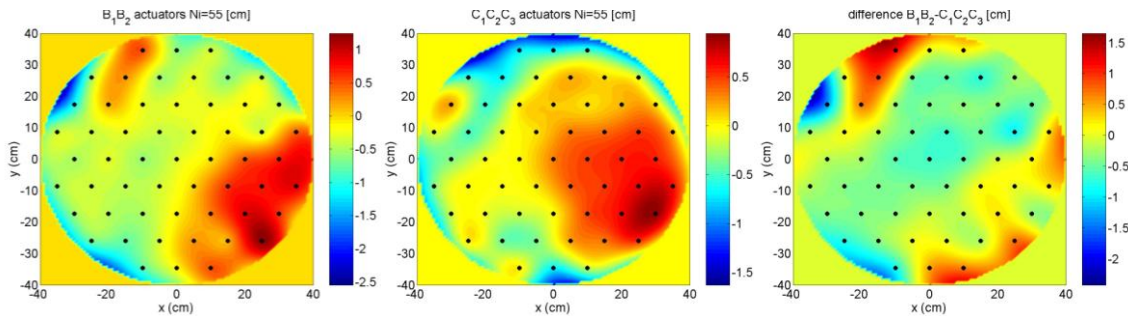
Figure 8. Shaped subreflector surfaces with 55 actuators relative to the parent ellipsoid in cm for the coverages B_1+B_2 and $C_1+C_2+C_3$ and difference between them.

SENSITIVITY ANALYSIS

With the purpose of modeling both the inaccuracy of the actuator positioners and possible thermo-elastic distortions, a random error uniformly distributed between [-0.1 mm, 0.1 mm] was added to the *z*-coordinates of the 55 actuators, and from these new sets of actuators the corresponding far-fields over the coverages were computed. A number of 1000 different runs was carried out on every coverage. Mean value, variance and standard deviation of the directivity loss observed over the coverages are reported in Table 5, while a plot of the results of the 1000 runs is given in Figure 9.

Table 5. Mean value, variance and standard deviation of the directivity loss on every coverage obtained from 1000 different runs.

	B_1B_2	$C_1C_2C_3$	D_1D_2
Mean value μ [dB]	0.2789	0.1928	0.1020
Variance σ^2 [dB^2]	0.0081	0.0047	0.0032
Standard deviation σ [dB]	0.0902	0.0687	0.0564

It is seen that variance, standard deviation and mean value of the directivity loss are somehow proportional to the dimension of the coverage.
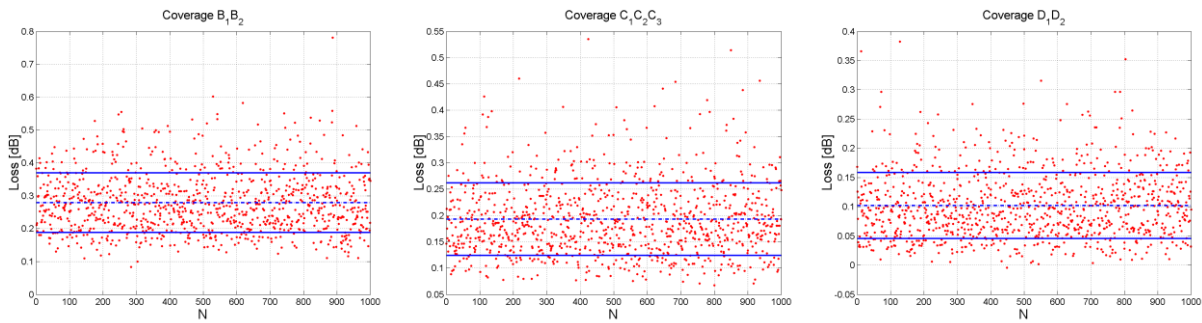
Figure 9. Directivity loss distribution on every coverage: μ (dashed line) and $\mu \pm \sigma$ (continuous line).

It was noticed however that the value of the loss reported in Figure 9 only affected a very limited number of stations over the coverages. It was seen that, on average, only 100 stations over B_1+B_2 (total stations =15025), 6 stations over $C_1+C_2+C_3$ (total stations=4905) and 4 stations over D_1+D_2 (total stations=3570) showed a loss, for all the five frequencies of interest, that was in the range [90% of max loss : max loss], with max loss being the directivity loss observed in Figure 9 for every run. This corresponded to the 0.67% of the total stations for Central Africa, the 0.12% for South Africa and 0.11% for Russia.

It was also seen that the number of stations in the interval [90% of max loss : max loss] diminished for an increase of max loss. For example, 144 stations of the coverage B_1+B_2 were in the range defined above if max loss was equal to 0.15 dB, while the number of stations decreased to 17 if max loss was 0.58 dB.

Moreover, it was observed that the stations in the range [90% of max loss : max loss] where all located at the border of the coverage, or in the area defined by the beam pointing error, and in most cases existed only for some frequencies. An example is given in Figure 10, where the contour levels 29 dBi and 25 dBi are plotted over Central Africa, for the nominal case with no random error and the case in which the maximum directivity loss is 0.48 dB. It is possible to see that contours are almost identical except for a change of the green curve at the northern border for one of the five frequencies. In this case, the number of stations on which the corresponding loss is in the range [90% of 0.48 dB: 0.48 dB] is 19.
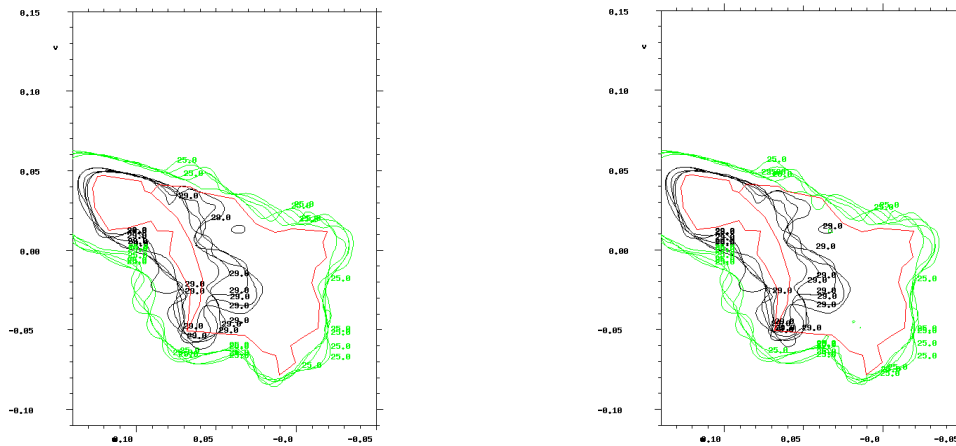
Figure 10. Contour levels 29 dBi and 25 dBi for the coverage B_1+B_2: on the left for no random error, on the right when the max loss is equal to 0.48 dB.

Finally, it was noticed that, by keeping fixed the random error distribution, there existed a linear behavior between the interval on which the random error was defined and the directivity loss observed.

Actuator free

The case of an actuator which is free to move was then taken into account. By removing the failing actuator from the set of the known actuators necessary for a given coverage, the new subreflector surface was computed and the effect on the radiated field was analyzed with POS5.

From the results presented in [4], the total forces at the actuators were computed and the actuator that showed the largest total force was then chosen and removed, see Figure 11. It was seen that directivities decreased by 1.17 dB over the coverage B_1+B_2, 1.13 dB over the coverage $C_1+C_2+C_3$ and 0.27 dB over D_1+D_2 relative to the nominal values reported in Table 4. It was also noticed that, when the actuator with total force equal to 0 N was removed, no loss in

directivity, as expected, was observed. As last test case, it was decided to consider free the actuator that lied in a location where the subreflector shaping varied across it, see Figure 11. It was seen that a loss in directivity existed also in this case, but that it was always smaller than the one observed for the actuator with the largest total force. It was thus concluded that the actuator with the largest total force was the most critical one for a free actuator failure and the responsible of the largest loss in the antenna performances.
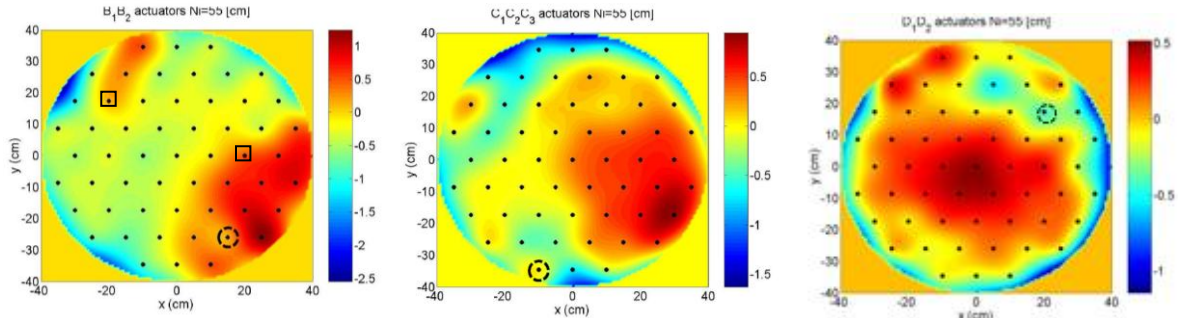
Figure 11. Position of the actuators with the largest force over the three coverages (circle with dashed line) and actuators on which the shaping varies across it (square with continuous line).

By removing the actuator that showed the largest force, a POS5 optimization was finally performed on the remaining 54 actuators to study the capability of the reconfigurable surface of compensating for a free actuator. The optimization showed that on each coverage it was possible to re-obtain the same directivity values reported in Table 4 for the nominal case: 54 actuators were thus able to compensate for a free actuator in the worst case.

Actuator stuck

The effect of an actuator that was stuck at a certain z-position, and thus could not be reconfigured, was then modeled. For a certain coverage, the control points were set to the expected z-values while the one that exhibited the largest z-variation in changing from the previous coverage was kept fixed. By doing that, the new subreflector surface was computed and its effect on the radiated field was analyzed with POS5.

The coverage $C_1+C_2+C_3$ and its difference relative to the coverage B_1+B_2 were considered, see Figure 12. One stuck actuator was assumed at a time. On the basis of the distance to the subreflector rim and the actuators z-variation in changing from B_1+B_2 to $C_1+C_2+C_3$ (see Figure 12, on the right), four cases were taken into account:

1. Actuator with difference larger than zero and close to the maximum value (circle).
2. Actuator with difference smaller than zero and close to the minimum value (triangle).
3. Actuator with difference larger than zero and located on the rim (square).
4. Actuator located at the centre of the subreflector (pentagon).
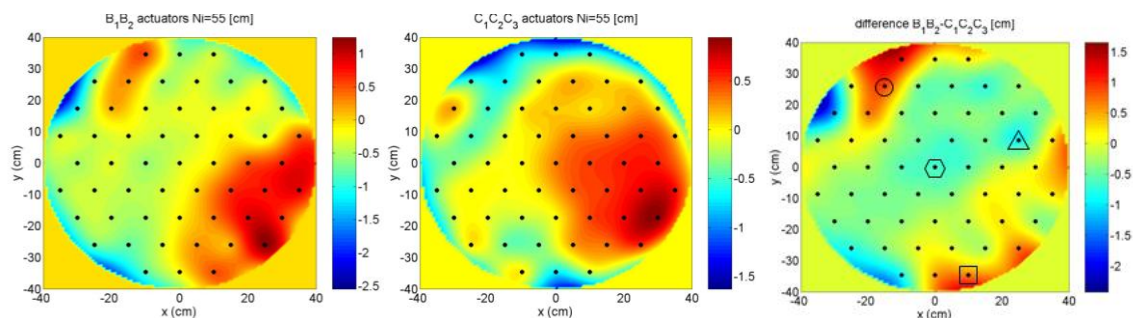
Figure 12. Shaped subreflector surfaces with 55 actuators relative to the parent ellipsoid in cm: on the left for the coverage B_1+B_2, in the middle for the coverage $C_1+C_2+C_3$ and on the right their difference.

While 54 actuators where set to the expected z-coordinates given by the coverage $C_1+C_2+C_3$, the actuator identified by the cases 1-4 was set to the z-coordinate defined by the coverage B_1+B_2 and the far-field was computed. It was seen that case 1 provided a loss in directivity equal to 1.99 dB, case 2 equal to 1.25 dB, case 3 equal to 0.43 dB and case 4 equal to 11.01 dB, relative to Table 4. It was concluded that the absolute value of the actuator z-difference and the distance of the actuator from the rim were important. In particular it was observed that a stuck actuator located on the rim had a much smaller effect on the antenna performances than one located at the center of the subreflector.

CONCLUSIONS

A dual reflector antenna constituted by a shaped and fixed main reflector and a reconfigurable subreflector designed for a realistic mission scenario in Ku band was investigated. The reconfigurable surface was modeled by a mesh of interwoven flexible wires with circular cross section and supported by a number of 55 control points. It was seen that the obtained directivity was 1.9 dB, over the largest coverage, and 1.2 dB, over the smallest coverage, lower than the best results given by a shaped, but fixed, dual reflector optimized for each individual coverage. At the same time, an improvement up to 2.9 dB could be obtained relative to a traditional fixed shaped reflector designed to illuminate the envelope of the coverages. The necessary number of actuators was studied and a sensitivity analysis to the actuator settings was then performed. It was seen that the inaccuracy of the actuator positioners and possible thermo-elastic distortions provided an average directivity loss in the [0.1 dB : 0.28 dB] range, depending on the considered coverage, but that this loss only influenced the 0.11% of the total stations of the smallest coverage and the 0.67% of the total stations of the largest coverage. The effects of an actuator which was stuck or free to move were finally studied. It was found that though a free actuator could provide a directivity loss up to 1.17 dB in the worst case, the remaining 54 actuators could successfully compensate for the failure with a new shaping. It was then observed that a stuck actuator located on the rim had a much smaller effect on the antenna performances than one located at the center of the subreflector.

REFERENCES

[1] K. Pontoppidan, "Reconfigurable reflector surfaces with imparted bending stiffness," *TICRA report S-582-02*, September 1994.
[2] R. C. Brown, P. J. B. Clarricoats, Z. I. Hai, "The performance of a prototype reconfigurable mesh reflector for spacecraft antenna applications," *Proceedings of the 19th European Microwave Conference*, September 1999.
[3] L. Datashvili, H. Baier, J. Schimitschek, M. Huber, "High precision large deployable space reflector based on pillow-effect-free technology," *Proceedings of the 48th Structures, Structural Dynamics and Materials Conference*, Honolulu, Hawaii, USA, May 2007.
[4] K. Pontoppidan, "Light weight reconformable reflector antenna dish," *Proceedings of the 28th ESA Antenna Workshop on Space Antenna Systems and Technologies*, Noordwijk, The Netherlands, June 2005.
[5] C. Cappellin, K. Pontoppidan, H.-H. Viskum , "Reconfigurable dual reflector for a realistic mission scenario in Ku band," *Proceedings of the 30th ESA Antenna Workshop on Antennas for Earth Observation, Science, Telecommunication and Navigation Space Missions*, Noordwijk, The Netherlands, May 2008.
[6] Homepage of POS5, http://www.ticra.com/script/site/page.asp?artid=6&cat_id=38, April 2008.